

Computerized Planning of Cryosurgery Using Cryoprobes and Cryoheaters

www.tcr.org

In a typical minimally invasive cryoprocure, multiple cryoprobes are inserted into the tissue with the goal of maximizing cryoinjury within a predefined target region, while minimizing cryoinjury to the surrounding tissues. A temperature-controlled electrical heater has been developed recently by this research team, in order to assist in limiting the cryoinjury to the target region. The new device has been termed a 'cryoheater,' and it can work with any cryosurgical cooling technique. A prototype computerized planning tool has been presented recently by this research team, which helps to determine the best locations in which to insert the cryoprobes. This prototype was designed for cryoprobes only. The planning procedure utilized a novel iterative optimization technique, based on a force-field analogy. The combination of cryoheaters with computerized planning is the subject matter of this report. The current report includes a review of cryoheater development, and presents an improved cryosurgery planning tool which incorporates cryoheaters.

Key words: Cryosurgery; Computerized Planning; Bioheat Transfer; Prostate; Cryoheater.

Introduction

Prostate cryosurgery was the first minimally invasive cryosurgical procedure to pass from the experimental stage and become a routine surgical treatment (1). The minimally invasive approach created a new level of difficulty in cryosurgery, in which a pre-defined 3D shape of tissue must be treated, while preserving the surrounding tissues. To overcome this difficulty, five (2) and six (Erbe Elektromedizin GmbH, Germany) minimally invasive cryoprobe setups were suggested during the early 1990's, based on liquid nitrogen cooling. With recent technological developments in Joule-Thomson cooling, the diameter of the cryoprobe has been dramatically decreased (Endocare, Inc., CA; Galil-Medical, Inc., Israel). In an effort to gain better control over the cryosurgical procedure, the number of cryoprobes has been increased to the point that more than a dozen cryoprobes can be applied simultaneously. If localized effectively, one of the potential benefits of the use of a large number of miniaturized cryoprobes is superior control over the freezing process. Naturally, the application of a large number of cryoprobes opens the door for debates over the cost effectiveness of such a procedure. Furthermore, using large numbers of cryoprobes may cause additional injury to the surroundings healthy tissues due to the insertion procedure. The clinical and technological complications of a cryoprocure with such a large number of cryoprobes may not be fully appreciated.

To date, cryoprobe localization is an art held by the cryosurgeon, based on the surgeon's own experience and rules of thumb. Cryoprobes are typically operated in a trail-and-error fashion, until the entire target area is thought to be frozen.

Yoed Rabin, D.Sc^{1,*}
David C. Lung, M.S.¹
Thomas F. Stahovich, Ph.D.²

¹Department of Mechanical Engineering
Carnegie Mellon University
Pittsburgh, PA 15213

²Department of Mechanical Engineering
University of California
Riverside, Riverside, CA 92521

* Corresponding Author:
Yoed Rabin, D.Sc.
Email: rabin@cmu.edu

Currently, there are limited means to determine the optimal locations or the optimal thermal history for the cryoprobes. Suboptimal cryoprobe localization may leave areas in the target region untreated, may lead to cryoinjury of healthy surrounding tissues, may require an unnecessarily large number of cryoprobes, may increase the duration of the surgical procedure, and may increase the likelihood of post cryosurgery complications, all of which affect the quality and cost of the medical treatment. Computerized planning tools would help to alleviate these difficulties, which is the subject matter of this research.

A prototype computerized cryoprobe localization tool has been presented recently by the current research team (3). The tool operates iteratively and relies on a series of bioheat transfer simulations of the cryosurgical procedure. In each iteration, a bioheat transfer simulation is used to predict the temperature distribution that would result from the current configuration of the cryoprobes. At the end of each simulation, defective regions are identified, where defects are defined as tissue outside the target area that was cryoinjured, or tissue inside the target area that was not cryoinjured. Using a force-field analogy, defective regions apply forces to the cryoprobes, moving them to better locations prior to the start of the next iteration. This process of simulation and cryoprobe displacement repeats until no additional improvement can be achieved. This force-field analogy technique has been proven numerically efficient in 2D, on representative cross sections of the prostate (3).

With the dramatic increase in the number of cryoprobes, a new challenge has been introduced to cryosurgery, which is how to restrict the destructive freezing effect to the target area. A good example of a device that prevents freezing to preserve desired tissues during cryosurgery is the so-called 'urethral warmer', routinely used in prostate cryosurgery. Technically, the urethral warmer is a counter flow, water heat exchanger, embodied in a standard catheter. The water, from a reservoir at close to core body temperature, is pumped through the catheter to maintain the urethra temperature above freezing. The urethral warmer has proven to minimize post cryosurgery complications associated with damage to the urethra (4). Unfortunately, the urethral warmer is the only warmer available today for assistance in cryosurgery control. Due to its large diameter and insertion technique, the counter-flow heat exchanger is limited to prostate cryosurgery.

The 'cryoheater', a new device for cryosurgery control, has been presented recently by this research team (5-7). The cryoheater is a temperature-controlled, electrical heater that can have either the shape of a minimally invasive cryoprobe, or the shape of the urethral warmer commonly used for prostate cryosurgery. Reports on a feasibility study and thermal analyses of the cryoheater have recently been pub-

lished (6, 7). In broad terms, cryoheaters can dramatically increase the ability to control the shape and size of the frozen region. However, a new level of difficulty in cryosurgery planning is introduced with the application of cryoheaters, because adding the heating elements to the already growing number of cryoprobes makes thermal visualization of the process a difficult task even for an experienced cryosurgeon or biothermal engineer. Effective use of cryoheaters requires the development of computerized planning tools, which combine cryoprobes with cryoheaters. It is our belief that the cryoheater will play a critical role in cryosurgery optimization and control.

Our long term goal is to develop a computerized planning tool for cryosurgery that takes a 3D reconstruction of a target region from an available imaging device, such as ultrasound or MRI, and suggests the best cryoprobe localization, based on bioheat transfer considerations. This computerized tool will include cryoheaters, and suggest their optimal number and preferred placement. To be useful, the tool must be able to perform full scale, 3D planning in a few minutes, while the patient is on the operating table. The current report includes a review of the cryoheater's development and a presentation of a prototype 2D cryosurgery planning tool, which incorporates cryoheaters.

The Cryoheater as a Means of Cryosurgery Control

To understand design requirement of cryoheaters, it is first necessary to evaluate the typical cooling power of cryoprobes. The idea of embedding heating elements in cryoprobes is not new (8-11). Rabin and Shitzer (11) have tested the incorporation of an electrical heater at the tip of a cryoprobe, in order to control the net cooling power of a cryoprobe *in vivo*. The cryoprobe suggested in (11) is based on liquid nitrogen cooling, where the liquid nitrogen flow rate is set to maximum at all times, and where the electrical heater is used to control the effective cooling power. This bulky cryoprobe, which had a diameter of 14 mm, produced a maximum cooling power of 80 W. A heating power of 160 W was needed to control its thermal performance.

Modern liquid nitrogen based cryoprobes can be made compatible with minimal invasive procedures. For example, Rabin *et al.* (12) developed a miniature cryoprobe, termed a 'cryoneedle,' in a configuration of two adjacent hypodermic tubes, having external diameters of 1.1 mm. The cryoneedle has been applied successfully in experimental cryosurgery on a sheep breast model (13). It has been shown that the particular design of the cryoneedle leads to a thermal efficiency as high as 43%, which means that 43% of the energy absorbed by the boiling nitrogen came directly from tissue freezing (the rest came from the surroundings and from the cryodevice). An average cooling power of 115W can be calculated from the experimental data presented in (12).

A common alternative for cryoprobe cooling is based on the Joule-Thomson effect, which is the sudden change in temperature as a result of a sudden change in pressure, when a gas flows through an expansion valve. From thermodynamics considerations, Joule-Thomson cooling creates a lower cooling power than liquid nitrogen boiling, in a comparable cryoprobe diameter. This is also evident by the lower operation temperature of liquid nitrogen-based cryoprobes. Nevertheless, due to other considerations, such as the feeding tube diameter and the heavy thermal insulation typically required for a liquid nitrogen-based system, the Joule-Thomson effect is currently considered superior by cryosurgical device manufacturers. It follows that the cooling power of a liquid nitrogen-based cryoprobe represents the upper limit for modern cryosurgical devices. Although frequently argued by cryosurgical device manufacturers, the superiority of one cooling technique over the other is more a hardware-promotion statement, rather than a scientific argument.

Contrary to common belief, the Joule-Thomson effect is not necessarily a cooling effect. At high initial temperatures, the Joule-Thomson effect generates heating. What constitutes a high initial temperature is specific to each gas, and is dominated by molecular parameters. This temperature varies significantly among gasses. For example, with an initial temperature near room temperature, and an initial pressure as high as a few thousand psi, Argon and Nitrous Oxide create cooling effects, while Helium creates a heating effect. This difference has been well appreciated by cryosurgical device manufacturers, and some cryodevices can go from a cooling mode to a heating mode simply by switching between different working gases.

If cryoprobes have the ability to heat, regardless of the cooling technique, using this capability to control the 3D shape of the forming ice ball could be considered. However, whether using electrical heaters imbedded in cryoprobes or using Joule-Thomson heating, the application of cryoprobes for heating is cumbersome in operation and expensive. Rabin *et al.* (5) have suggested the cryoheater as an alternative device for heating during cryosurgery. Figure 1(a) shows a schematic illustration of a minimally invasive cryoheater, which has comparable dimensions to a standard minimally invasive cryoprobe.

The upper limit of the heating power required from a cryoheater can be approximated as the negative of the cooling power of a cryoprobe, as reviewed above. In this case, if the cryoheater and a cryoprobe are placed in exactly the same location, the cryoheater will neutralize the cryoprobe cooling effect. However, the minimally invasive cryoheater is design to assist in shaping the frozen region, where the cryoheater would obviously be localized close to the edge on the ice ball. This would dramatically decrease the heating power demands on the cryoheater. Based on elementary

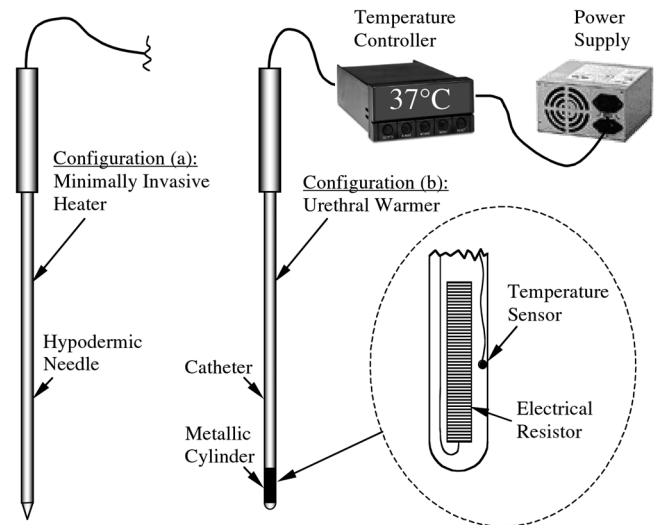


Figure 1: Schematic illustration of the cryoheater setup in two configurations: (a) a minimally invasive heater, having comparable dimensions to a minimally invasive cryoprobe (21, 25), and (b) a flexible urethral warmer (21, 23).

steady state heat transfer calculations for example, less than 1.2 W will be required to maintain a minimally invasive cryoheater at 37 °C, under the following conditions: a cryoheater diameter of 1 mm, a cryoheater active length of 10 mm, the cryoheater is surrounded by a large number of cryoprobes at a radius of 10 mm from the center of the cryoheater, the cryoprobes' temperature is -145 °C (typical of Argon cooling), and the average thermal conductivity of the frozen region is 2 W/m·°C. Such a low heating power requirement can hardly justify the use of cryoprobes having heating capabilities, but it can easily justify the development of simple and inexpensive heating elements such as the cryoheater, which can be constructed using off-the-shelf electrical resistors and a low power electrical source.

Figure 2 presents results from a feasibility testing of the cryoheater as a urethral warmer (see also Fig. 1(b)). As a urethral warmer, the cryoheater is inserted into the urethra as a catheter. The purpose in this heating application is to preserve the urethral wall. It can be seen from Figure 2(d) that an unfrozen region, having a thickness of 0.8 mm, can be preserved around the cryoheater as a urethral warmer.

The superiority of the cryoheater as a urethral warmer is discussed by Rabin and Stahovich (6), however, clinical support for that discussion is yet not available. Figure 3 shows a parametric study for the resulting temperature of the outer wall of the currently available urethral warmer, which is based on a counter flow heat exchanger. This parametric study is presented for an inner wall temperature of 37 °C and for various wall thicknesses. A wall thickness of 0.1 mm may be considered extremely thin, and a wall thickness of 0.5 mm may be considered practical. In either case,

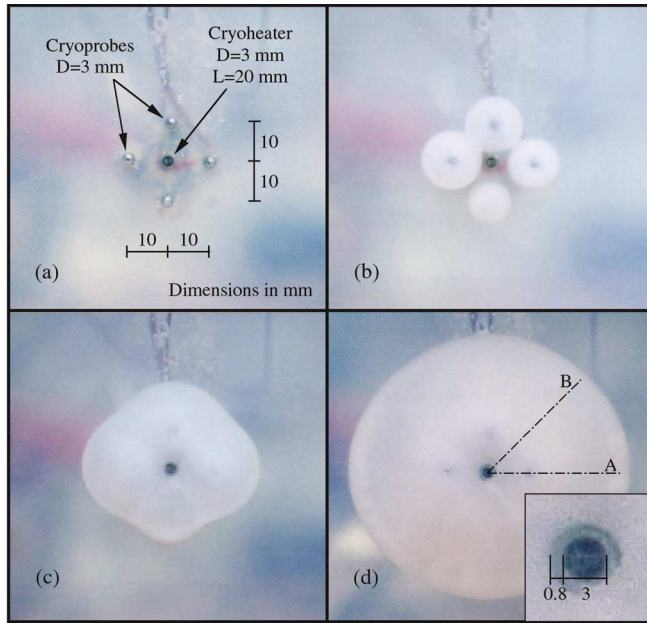


Figure 2: Feasibility testing of a cryoheater application in a gelatin solution, as presented in detail by Rabin and Stahovich (25). The particular experimental system was designed to generate a 2D heat transfer process, simulative of urethral warming during prostate cryosurgery (see also Fig. 1(b)). Images are taken (a) before the beginning of the experiment, (b) after 1 min, (c) after 4 min, and (d) 10 min from the beginning of cryoprobes activation.

freezing at the outer surface of the urethral wall is expected if the cryoprobes are placed too near to the urethra. The curve of zero wall thickness refers to the cryoheater as a urethral warmer. This effect is taken into consideration in the results and discussion section of this report.

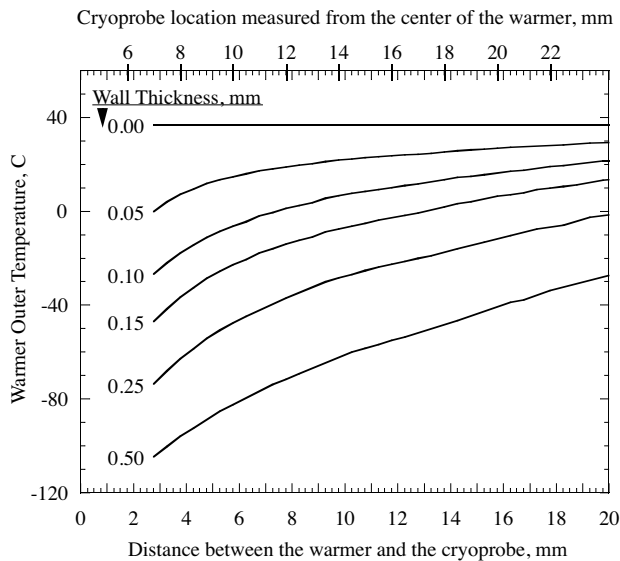


Figure 3: Outer wall temperature of a urethral warmer, based on 2D steady state heat transfer simulations (23). The urethral warmer diameter is 5 mm and it is surrounded by six equidistant cryoprobes at -145 °C.

Computerized Planning of Cryosurgery

In typical conditions of cryosurgery, cryoinjury starts to take place a few tenths of a Celsius degree below 0 °C, with the onset of crystal formation, while the phase transition in biological tissues takes place over a wide temperature range, depending on the composition of the biological solutions; this range can be as wide as 22° C, if the biological solution is first order-approximated as an NaCl solution (14). Maximum destruction is widely assumed to be below the lethal temperature, commonly taken as -45 °C. The debate about the actual value of this temperature is as long as the history of cryosurgery. Other possible values of the lethal temperature were reviewed by Baust and Gage (15), and a discussion on the severe uncertainties associated with measuring this temperature threshold in a clinical setup was given in (16). Other effects are known to be associated with cryoinjury (15, 17), such as the cooling rate during freezing, the rewarming rate, the age of the patient, and pre-exposure to other therapy. Today, many cryosurgeons consider temperature to be the single most important parameter indicating cryoinjury, probably because the temperature field can be relatively easily associated with the image of the frozen region, when using standard imaging techniques such as ultrasound and MRI. The goal in a minimally invasive cryoprocurement is to maximize the cryoinjury in a 3D target region, while minimizing cryoinjury to the surrounding tissues. Since the temperature distribution is a continuous field, maximizing internal cryoinjury while minimizing external injury represents contradicting requirements. Hence, an optimal planning of a cryoprocurement includes an acceptable balance between the above contradicting effects.

In broad terms, the objective of an acceptable balance between maximum internal injury and minimum external injury can be achieved by two complimentary processes: planning and control. Planning is the subject matter of the current report, and is independent of the cooling hardware. Control is hardware specific, and it is related to a feedback control system, which leads to an interaction between the desired and the actual temperature fields. It is well established that control alone cannot lead to an optimal cryosurgical result, since the frozen region formation is limited in size and rate of growth, which in turn are unique to the specific cryodevice and cryoprobes. The underlying assumption in the current research is that optimal planning is a necessary requirement for achieving the desired outcome from cryosurgery. However, optimal planning alone may be insufficient, due to the interaction between the cryodevice and the far more complicated thermal regulation system of the human body. For example, as a response to localized cooling, the thermal regulation system of the body may increase blood flow in an effort to compensate for the imposed cooling. At a later stage, the thermal regulation system may

decrease blood flow, in order to conserve energy, as is typical in long-term exposure to a cold environment. Hence, cryodevice control is necessary in order to compensate for differences between planning in a simplified mathematical world and the outcome of cryosurgery in the real world. The current study addresses optimal planning only, leaving control to the manufacturer of the specific cryodevice.

A prototype computerized planning tool for a multiprobe cryoprocure, termed the ‘Cryoplanner’, has recently been presented (3). The prototype has been demonstrated on a 2D case, illustrative of a typical cross section of prostate cryosurgery. Parametric studies with that cryoplanner have demonstrated that the technique is at least an order of magnitude more efficient than traditional optimization techniques for the same problem. Parametric studies also demonstrated that a good final configuration can be found regardless of the quality of the initial configuration. The current report presents, for the first time, a prototype computerized planning tool, which combines the operation of both cryoprobes and cryoheaters.

Related Work

Keanini and Rubinsky (18) reported on a numerical optimization technique for prostate cryosurgery planning. In that study, the task was to optimize the number of cryoprobes, their diameter, and their active length. Thus, there were three variables to be optimized. The prostate was modeled as a truncated cone with the urethra as a coaxial cylinder. The locations of the cryoprobes were determined by first dividing the prostate into a number of equiangular sub regions equal to the number of cryoprobes. One cryoprobe was placed at the centroid of each such subsection. The resulting configuration was a set of cryoprobes placed at equal intervals along the circumference of a circle. The study employed a 3D transient heat transfer simulation. The quantity minimized was the ratio of the volume of the frozen extraprostatic tissue to the volume of the prostate, evaluated at the time when the entire prostate becomes frozen. This study assumed symmetry and constant material properties in order to reduce simulation costs. In the current study, we consider asymmetric geometry and material properties that depend on temperature.

The study in (18) employed the simplex optimization method, which proved to be well suited to the problem formulation used there. In general, the simplex method is known to work well for problems that are linear, or nearly so (19, 20). In our study, we optimize the location of the cryoprobes and cryoheaters. This results in a highly non-linear problem, for which the simplex method is unlikely to be effective. In addition, there are significantly more variables to optimize. Keanini and Rubinsky suggest that if other optimization techniques are used for problems such as the one they studied,

those methods that compute explicit derivatives are likely to be inefficient. Our work employs a novel technique that avoids calculating derivatives in order to minimize the number of simulations needed for each step of optimization.

Baissalov *et al.* (21) have also presented a model for cryosurgical planning. In this model, a thermal simulation algorithm was used to generate temperature distribution around cryoprobes, visualize isotherms in the anatomical region of interest, and provide tools to assist estimation of the amount of freezing damage to the target region and surrounding normal tissues. The thermal simulation was based on solving the transient heat conduction equation using finite element methods. The optimization work in (21) was semi-empirical, while the optimization technique presented here is driven solely by bioheat transfer considerations. Unlike the work presented in (21), the technique presented in the current report is fully automated.

In a following report, Baissalov *et al.* (22) demonstrated that it is possible to simultaneously optimize multiple cryoprobe placements and their thermal protocol for one freeze-thaw cycle. The gradient descent method was used for the purpose of the study presented in (22), while our work employs a novel technique that avoids calculating derivatives, and is therefore more efficient. Three different forms of objective function were examined in (22), and it was found that the optimization results were dependent upon the initial values of the variables, the form of the objective function, optimization goals, and the mathematical method adopted for gradient calculation. By contrast, we have demonstrated (3) that the end result of planning – using the optimization algorithm we developed – is quite robust and independent of the above.

Numerical Simulations

The planning process is based on a sequence of bioheat transfer simulations of the cryoprocure. The numerical simulation scheme used for the current cryoplanning tool has been developed by Rabin and Shitzer (14), and is presented here briefly. For each step of optimization it is necessary to compute a single bioheat transfer simulation of the cryoprocure. It is customary to assume that heat transfer in the presence of blood perfusion can be modeled by the classical bioheat equation (23):

$$C \frac{\partial T}{\partial t} = \nabla \cdot (k \nabla T) + \dot{w}_b C_b (T_b - T) + \dot{q}_{met} \quad [1]$$

where C is the volumetric specific heat of the tissue, T is the temperature, t is the time, k is the thermal conductivity of the tissue, \dot{w}_b is the blood perfusion rate (measured in volumetric blood flow rate per unit volume of tissue), C_b is the volumetric specific heat of the blood, T_b is the blood temperature entering the thermally treated area (typically the core

body temperature), and \dot{q}_{met} is the metabolic heat generation. Note also that metabolic heat generation is typically negligible compared to the heating effect of blood perfusion and is therefore neglected in this study (24).

The scheme used here to solve Eq. [1] is based on a finite difference formulation:

$$T_{i,j,k}^{p+1} = \frac{\Delta t}{\Delta V_{i,j,k} [C_{i,j,k} + (\dot{w}_b C_b)_{i,j,k} \Delta t]} \sum_{l,m,n} \frac{T_{l,m,n}^p - T_{i,j,k}^p}{R_{l,m,n-i,j,k}} + \frac{\Delta t [(\dot{w}_b C_b)_{i,j,k} T_b + (\dot{q}_{met})_{i,j,k}] + C_{i,j,k} T_{i,j,k}^p}{C_{i,j,k} + (\dot{w}_b C_b)_{i,j,k} \Delta t} \quad [2]$$

where i,j,k and l,m,n are space indexes, p is a time index, ΔV is an element unit volume, Δt is a time interval, and R is the thermal resistance to heat transfer between grid point i,j,k and its neighbor l,m,n . We implement Eq. [2] on a rectangular grid of points. The numerical scheme described in Eq. [2] is conditionally stable, and a discussion regarding its applicability for cryosurgery has been presented by Rabin and Shitzer (14).

Table I lists typical values of the thermophysical properties of biological tissues, which were used in this study. Recently, Rabin (25) studied how uncertainties in these thermophysical properties propagate through bioheat transfer simulations.

The Cryoplanner

In the course of the current presentation, the term ‘cryoelement’ is used as a generic term, meaning either a cryoprobe or a cryoheater. Our technique employs the notion of an objective function, however, it is not used in the traditional manner. Our objective function is a measure of the total defect area, where defects are regions in the target area that have not been cryoinjured, and regions in the surrounding healthy tissues that have been cryoinjured. Rather than using the numerical value of the objective function to directly derive the optimiza-

tion, we employ a force-field analogy based on the individual defect regions. These defects apply forces to the cryoelements, tending to move them to locations that would reduce the value of the objective function. For our method, there is no need to compute gradients of the objective function.

Our objective function also serves a second role, which is determining the best outcome possible for a given configuration of cryoelements. Once a configuration is selected, it is necessary to determine how long to run the procedure, i.e., how long the cryoprobes should be activated. If the cryoprobes are not operated long enough, some portions of the target region that could have been treated will not be. Conversely, if the cryoprobes are operated too long, healthy surrounding tissue will become cryoinjured. To determine the correct operating time, our software continually monitors the value of the objective function while computing the bioheat transfer simulation. When the value of the objective function reaches its minimum, the simulation is terminated. The time of termination is the optimal procedure time for that particular configuration of cryoelements, however, that configuration may not be the optimal configuration.

An ideal configuration of cryoelements would result in no defects. However, for the typical number of cryoprobes used in practice, the ideal solution is generally not achievable. Our approach searches for the minimum area of defects achievable for a specified number of cryoprobes, chosen by the cryosurgeon. If the best configuration is inadequate, cryoheaters are added and optimized by the cryoplanner. With the introduction of cryoheaters, we hope to limit the size of external defects, and to allow the cryoprobes greater operation time to minimize the size of inner defects.

The Objective Function

In general, the choice of objective function (the quantity to be minimized), dictates the quality of the solutions that can be found, and the speed with which they are obtained. The objective function in this study, G , is the sum of all of the defect areas:

Table I
Representative thermophysical properties of biological tissues used in the current study (T in degree K) (6, 7, 26).

Thermophysical Property	Value	
Thermal conductivity, k , W/m-K	0.5	$273 < T$
	$15.98 - 0.0567 \times T$	$251 < T < 273$
	$1005 \times T^{-1.15}$	$T < 251$
Volumetric specific heat, C , kJ/m ³ -K	3600	$273 < T$
	15,440	$251 < T < 273$
	$3.98 \times T$	$T < 251$
Latent heat, L , MJ/m ³	300	
Blood perfusion heating effect, $w_b C_b$, kW/m ³ -K	40	

$$G = \int_A w \, dA \cong \sum_m w_m A_m \quad [3]$$

where A is the total area of the simulated problem, including both the target area and the surrounding tissue, w is a defect weighing function based on temperature, and m is an index representing all numerical grid points in the simulated 2D domain.

To evaluate the objective function, it is necessary to first define the temperature ranges that constitute defects in the solution. As discussed above, one may wish to have all of the tissue in the target region be below $-45\text{ }^\circ\text{C}$, which is the commonly accepted lethal temperature. One may further wish all of the tissue outside the target region to be above $0\text{ }^\circ\text{C}$, which is the lowest temperature before the destructive effect of ice crystallization is initiated. However, due to the physics of freezing, it is not possible to achieve such a step like change in temperature at the boundary of the target region (6, 7). Thus, even the best possible solution would have a significant defect area consisting of the tissue between the $0\text{ }^\circ\text{C}$ and the $-45\text{ }^\circ\text{C}$ isotherms. The size of this transition region is dictated, to a large extent, by the thermophysical properties of the tissue. The transition region size could be reduced with the presence of cryoheaters, but it cannot be completely eliminated.

A clinical approach to this problem may be to match either the $0\text{ }^\circ\text{C}$ or the $-45\text{ }^\circ\text{C}$ isotherm with the contour of the target region, creating the so-called “safety margins” interior or exterior to the target region, respectively. An alternative approach would be to allow the planning algorithm to split the area of the transition region between the target area and the healthy surrounding tissues. In the studies presented here, the $-22\text{ }^\circ\text{C}$ isotherm was chosen as the temperature isotherm for optimization, which results in an almost exact split of the defect area between the target region and the surrounding healthy tissues. It is emphasized that any temperature isotherm could be used instead with our software. Ultimately, it will be the decision of the clinician whether the safety margins should be interior to the target region, exterior to the target region, or distributed between the interior and exterior regions. Accordingly, the defect weighting function is defined as follows:

$$w_m = \begin{cases} 1 & -22\text{ }^\circ\text{C} < T_m & \text{interior to the target area} \\ 0 & T_m < -22\text{ }^\circ\text{C} & \text{interior to the target area} \\ 1 & T_m < -22\text{ }^\circ\text{C} & \text{exterior to the target area} \\ 0 & -22\text{ }^\circ\text{C} < T_m & \text{exterior to the target area} \end{cases} \quad [4]$$

where T_m is the temperature at grid point m .

The objective function, G , Eq. [3], also serves as the criterion for terminating the bioheat transfer simulation of the cryopro-

cedure. As described above, the value of G is monitored during the simulation to determine the minimum value achievable for that configuration of cryoprobes. At the beginning of any simulation, the entire target region would be at core body temperature, thus the value of G would equal the area of the target region. In the early stages of freezing, the interior defect area would decrease with time, as would the value of G . At a more advanced stage, freezing would begin to extend beyond the boundaries of the target region, and exterior defect regions would start to form. When the growth rate of the exterior defect regions matches the rate of decrease of the interior defect regions, the total volume of defects would be at its minimum value. At this point, the cryosurgery simulation is terminated, and G has the smallest value possible for that configuration of cryoelements. Note, that this may not be the minimum value of the objective function, as other cryoelements configurations may produce smaller values.

Force-Field Analogy

The primary issue for this optimization technique is to determine how to move the cryoelements to achieve smaller values of the objective function. Rather than traditional optimization techniques, which would require partial derivatives of the objective function with respect to the coordinates of the cryoelements, the defects in the temperature field are used to directly drive the cryoelement to improved locations. The total force applied by the temperature field to a cryoelement is given by:

$$\vec{F}_{nT} = \sum_m \frac{C_1 C_2}{|\vec{r}_{mn}|^q} w_m A_m \Delta T_m \vec{u}_{mn} \quad [5]$$

where \vec{F}_{nT} is the net force vector applied to cryoelement n by all of the defects; C_1 is a device constant related to the cooling capability of the cryoprobe; C_2 is a parameter indicating the cryoelement type, having a value of 1 for a cryoprobe (generating attraction forces to internal defects, and repulsion forces from external defects) and a value of -1 for cryoheaters (generating repulsion forces from internal defects, and attraction forces to external defects); w_m is the weight function in Eq. [4]; A_m is the cross sectional area associated with grid point m ; ΔT_m is the difference between the temperature threshold for optimization and the temperature at grid point m , i.e., $\Delta T_m = (-22\text{ }^\circ\text{C}) - T_m$; \vec{r}_{mn} is a vector from grid point m to probe n ; \vec{u}_{mn} is a normalized version of \vec{r}_{mn} ; and q is the power at which the force falls off with the distance, having a value of 2 and 3 for cryoprobes and cryoheaters, respectively.

The force formulated in Eq. [5] falls off rapidly with distance, so that defects near a cryoelement apply larger forces than defects farther away. The rationale is that the cryoelement nearest a defect are likely to have the largest influence on that

defect. For cryoheaters, the force applied by each defect falls off faster than for cryoprobes, which was found to be efficient from parametric studies. Either way, the force applied by a defect is also proportional to the temperature difference, ΔT_m . This allows defect areas with more significant temperature differences (i.e., more significant defects) to apply larger forces, thus accelerating the optimization process.

In order to prevent congestion of many cryoelements at the same location, a short acting repulsive force is applied between all cryoelements:

$$\vec{F}_{nP} = \sum_j \frac{C_3}{|\vec{r}_{jn}|^3} \vec{u}_{jn} \quad [6]$$

where \vec{F}_{nP} is the net force vector applied to cryoelement n by all of the other cryoelements, j is the cryoelement index, C_3 is a constant, \vec{r}_{jn} is a vector from cryoelement j to cryoelement n , and \vec{u}_{jn} is a normalized version of \vec{r}_{jn} . This force is inversely proportional to the cube of the distance between probes so that the force is negligible unless the probes are very near one another.

Moving Cryoelements

When a cryoelement is selected to be moved by our planning algorithm, it is moved in proportion to the net force it experiences:

$$\Delta \vec{r}_n = C_0 (\vec{F}_{nT} + \vec{F}_{nP}) \quad [7]$$

where $\Delta \vec{r}_n$ is the displacement and C_0 is a constant. Examining Eqs. [5]-[7] indicates that there are a total of three constants influencing this displacement: C_0 , C_1 , and C_3 . However, the constants appear only in products, and thus only two quantities matter: $C_{01}=C_0C_1$ and $C_{02}=C_0C_3$. For cryoprobes, the values used for these quantities are 2×10^{-11} and 1.2×10^{-10} , respectively. For cryoheaters, the values used for these quantities are 2×10^{-13} and 1.2×10^{-14} respectively. These values were obtained empirically, and have been found to work well in practice. Using larger values results in larger displacements of the cryoprobes, which could accelerate the solution, but may cause the optimizer to overshoot the optimum configuration and terminate prematurely. Using smaller values has the opposite effect.

To be consistent with the grid representation used for computing the bioheat transfer simulations, before the cryoprobes are displaced, $\Delta \vec{r}_n$ must be rounded to the nearest grid cell location. Furthermore, to prevent overshooting the optimum, the maximum displacement is limited to three grid cells in the x and y directions. This is a conservative choice that was obtained empirically and has proven to work well.

Clinical constraints also govern the cryoprobe displacements. For example, in the current study cryoprobes are not permitted to be displaced outside the target region, they are not permitted to be placed in the urethra during prostate cryosurgery, and they are not permitted to be closer than 2 mm to the boundaries of the target region. Since the primary purpose of cryoheaters is to minimize outer defects, cryoheaters are only placed outside the target region.

It is possible to move multiple cryoprobes on each iteration of optimization as a means of accelerating the solution process. However, if too many are moved simultaneously, it is believed that the optimizer could miss the optimum and terminate prematurely. Our approach is to move multiple cryoprobes when the defect area is large, and to move them one at a time otherwise. If the total defect area is less than 1/8 of the area of the target region, only the cryoprobe with the largest force (i.e., $\Delta \vec{r}_n$ the largest value of) is moved. If the total defect area is larger than this, the three cryoprobes with the largest forces are moved. In the case of cryoheaters, only one cryoheater is moved at a time, and only one grid cell at a time. This is due to the smaller number of cryoheaters that are typically added to the configuration as well as the smaller radius of influence cryoheaters have in comparison to cryoprobes. This scheme is based on empirical observations of our system. We have found this scheme to work well; however, it may be possible to move cryoelements more aggressively without missing the optimal solution.

Planning Strategy

One approach to planning would be to optimize all of the cryoelements, both cryoheaters and cryoprobes, simultaneously. According to our experience, however, we have found that this is inefficient. Instead, we find the optimal solution using only cryoprobes, and then add cryoheaters only when necessary. When planning with cryoheaters, we use a two step process in which the cryoprobes are optimized first, with the cryoheaters kept stationary, followed by a cryoheater optimization with the cryoprobes held stationary. Cryoheaters are added by the optimizer one at a time, depending on the results of each step of planning.

To begin the optimization process with cryoprobes, it is necessary to select an initial configuration. For example, cryoprobes can be randomly distributed within the target region, or the user can manually select a preferred initial configuration, based on his or her own clinical experience. (We have shown previously (3), however, that the outcome in the absence of cryoheaters is insensitive to the initial condition.) Next, a bioheat transfer simulation is computed until the optimal termination time is reached. Then the forces on the cryoprobes are computed and one or more cryoprobes are moved accordingly. This provides the configu-

ration for the next iteration. Ordinarily, the process repeats in this fashion for many iterations.

Eventually, an iteration will result in an increase, rather than a decrease, in the total defect area. This typically occurs when the configuration is nearly optimal, and the particular cryoprobe moved was already at an (locally) optimal location. Because this occurs when the solution is nearly optimal, the iteration typically involves moving just one cryoprobe. When this happens, the program begins a backtracking procedure. The iteration is rejected, and the cryoprobe that had the second largest force in the previous iteration is moved. If this again results in an increase in the defect area, the program again backtracks, this time moving the cryoprobe with the third largest force. Backtracking continues until either an improvement is achieved or the program backtracks through all of the cryoprobes. In the former case, the program continues on in the usual way. In the latter case, a local optimum has been found for the given number of cryoprobes.

Now the program checks if the best value of the objective function achieved during cryoprobe optimization, $G_{min,overall}$ (Eq. [3]) is below a certain threshold, $G_{cryoheaters}$ (5% of the total target area in the current study). If $G_{min,overall}$ is greater than $G_{cryoheaters}$, the planning program starts to add cryoheaters, otherwise the program terminates. The decision whether or not to add cryoheaters is made in the Alternate Cryoelements Optimization block of Figure 4.

If a decision is made to add a cryoheater, the program determines the location of the outer defect that extends the farthest from the target boundary, and places a cryoheater in the grid cell nearest the center of the defect. Now that a cryoheater has been added, planning resumes.

At the end of this two-step procedure, the program checks again if the objective function has reached a low enough value, i.e., if $G_{min,overall} > G_{cryoheaters}$. If $G_{min,overall}$ is still greater than $G_{cryoheaters}$, another cryoheater is added and the two-step optimization procedure is repeated. The process may continue for many optimization cycles. However, to make sure that the program will not run endlessly, the program terminates planning if the number of cryoheaters exceeds the number of cryoprobes. While cryoheaters are yet not used clinically, and while general rules on the number of cryoheaters are yet not available, we believe that a number of cryoheaters greater than the number of cryoprobes is not likely to be used. When the planning process terminates, the program reports the optimal coordinates of the cryoelements. It also reports the optimal coordinates computed each time a cryoheater was added. Ultimately, the acceptable overall defect size for a given number of cryoheaters, will be the clinician's decision, as discussed below.

Results and Discussion

For the purposes of the current report, the planning algorithm was demonstrated in 2D, on a cross sectional area typical of a prostate, as illustrated in Fig. 5. The following parameters were used in this study:

- (I) The cryoprobe temperature was idealized by assuming a step-like temperature change at the beginning of the process, dropping from 37 °C to -145 °C, where -145 °C is a typical operation temperature of Joule-Thomson cryoprobes working on Argon gas. In practice, it takes about 30 seconds for such a cryoprobe to reach the lowest working temperature (tracing a specific cryoprobe performance is not deemed worthwhile for the purpose of the development of the cryoplanner).
- (II) The cryoheater temperature was maintained at 37 °C for the duration of the optimization.
- (III) The cryoprobes and cryoheaters had an external diameter of 1 mm.
- (IV) The diameter of the urethra was assumed to be 6 mm (equals $2R_2$ in Fig. 5). Consistent with current clinical applications of urethral warmers, the urethra was maintained at a temperature of 37 °C throughout the simulated operation (4, 15).
- (V) The average prostate volume is in the range of 25 and 50 ml, where the difficulty in limiting freezing to the target region increases with a decrease in volume of the target region. Two extreme cases of prostate diameter ($2R_0$ in Fig. 5) were studied: 30 mm and 56 mm, corresponding to a spherical volume of about 15 ml and 50 ml, respectively. Of course, this is an idealized geometry, used only to study the cryoplanner capabilities.
- (VI) The urethra was off center by 8 mm ($R_1=8$ mm in Fig. 5), thus providing a more anatomically realistic problem.
- (VII) The values used for the thermophysical properties are listed in Table I.
- (VII) The simulated cross sectional area, including the prostate and surrounding healthy tissues, was 120 mm × 120 mm. Due to symmetry, only half of this cross section was simulated. A zero heat flux thermal boundary condition was imposed on the outer perimeter of the simulated cross section (not on the perimeter of the target region). For the duration of

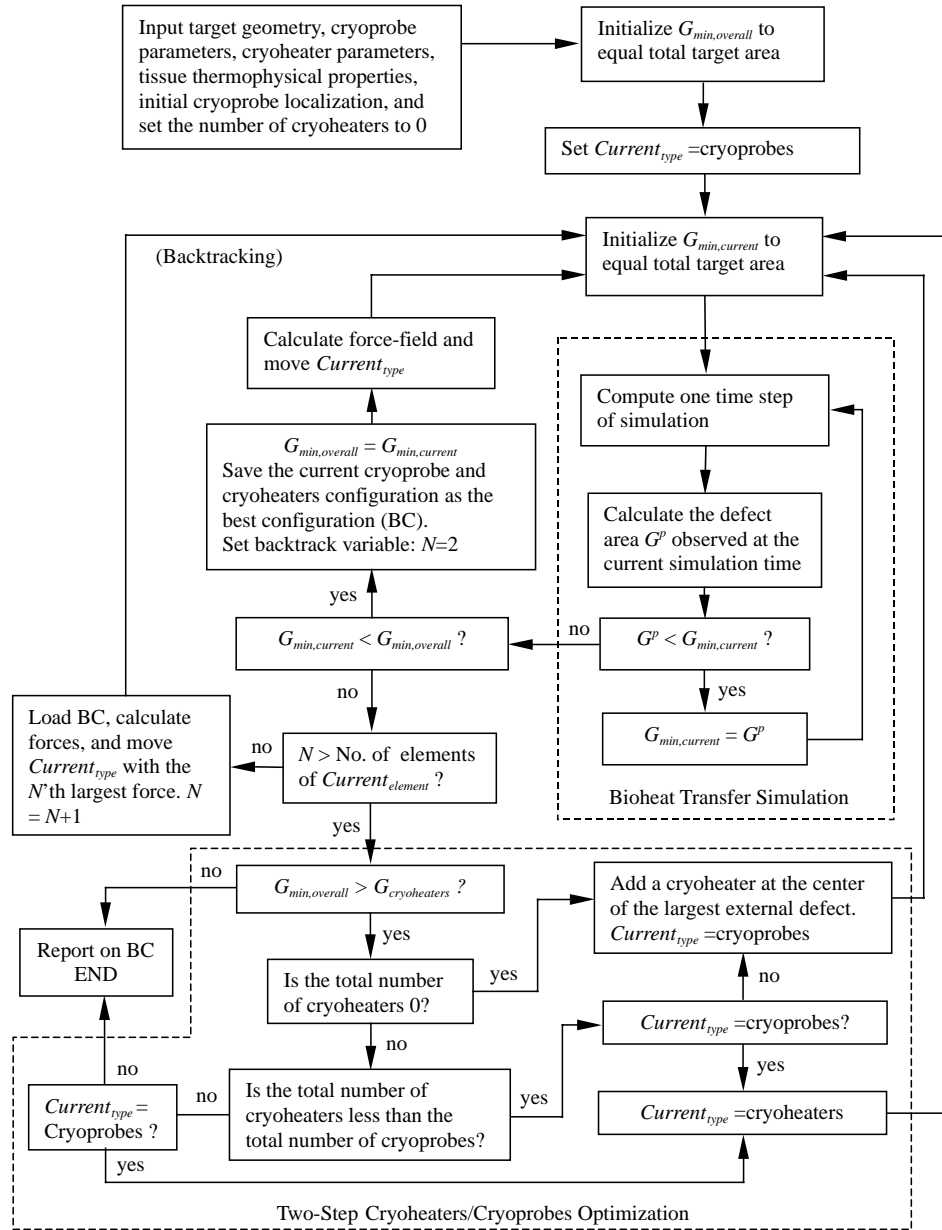


Figure 4: Planning algorithm: G^p is the objective function presented in Eq. [3], evaluated at time level p of the bioheat transfer simulation; $G_{min,current}$ is the minimum value calculated up to time level p for the current configuration of cryoprobes; $G_{min,overall}$ is the minimum value of $G_{min,current}$ from all configurations tested up to the current iteration of planning; N is a cryoelement

index in the backtracking process; $G_{cryoheater}$ is the threshold above which cryoheaters are added in search for an optimum configuration; BC is the best cryoelement configuration. The planning algorithm optimizes either cryoprobes or cryoheaters at a specific cycle of planning, where $Current_{type}$ indicates the current cryoelement type.

the simulated procedure, the temperature at the outer boundary was found to be unchanged from its initial temperature, indicating that the domain could be considered infinite from heat transfer consideration. For computing bioheat transfer simulations, a 1 mm × 1 mm grid was used.

(IX) Two cryoelement placement cases were studied, in the presence and absence of a standard place-

ment grid of 5 mm. (A placement grid is metal plate with holes in it, which a cryosurgeon use to select insertion locations.) In the absence of the placement grid, cryoelements were permitted to be placed at any numerical grid point. In the presence of the placement grid, cryoelements were allowed to be placed in 5 mm intervals in x and y along the numerical grid (where z represents the cryoprobe axial direction). This leads to

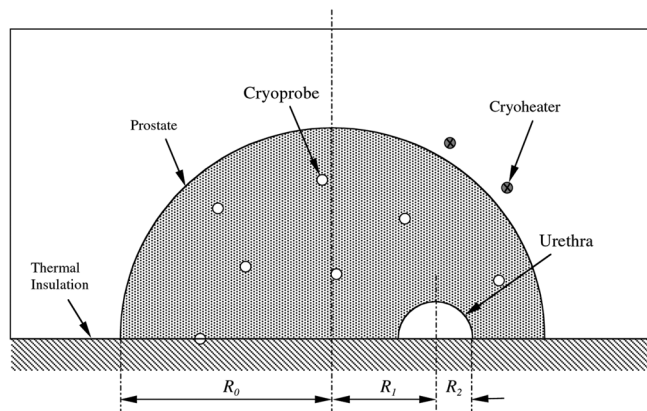


Figure 5: Schematic illustration of the idealized prostate cross section used for the Cryoplanner demonstration. Because of symmetry, only half of the cross section was considered in the bioheat transfer simulation.

a significant reduction of possible cryoelements locations within the prostate.

- (X) In order to accurately identify the defect regions, the numerical grid used to compute the bioheat transfer simulations was interpolated. Each 1 mm × 1 mm grid cell was divided into 100 sub-cells, each 0.1 mm × 0.1 mm. The temperatures on this finer grid were interpolated from the values on the larger grid using bilinear interpolation. In this report, index *m* in Eqs. [3]-[5] refers to this finer grid.
- (XI) The initial cryoprobe placement was uniform distribution in the cross section, which leads to a relatively shorter optimization process (3).

Table II lists the total defect area size for all cases studied in this report. Figures 6-8 present results of planning in the

absence of a placement grid, where cryoelement placement is permitted at any numerical grid point. Three shades of gray are shown in Figures 6-8: The dark gray represents the region with temperatures below -45 °C, the intermediate gray represents the region with temperatures between -45 °C and -22 °C, and light gray represents the region with temperatures between -22 °C and 0 °C.

Figure 6 shows the optimization process in a typical case of 5 cryoprobes. Figure 6(a) shows the optimal solution without cryoheaters, which required a total of 6 iterations (including backtracking). Now, that the optimal cryoprobe placement has been obtained, the algorithm adds either one or two cryoheaters at the center of the largest external defect (one if the cryoheater is placed on the symmetric line or two otherwise). Next, the cryoplanner optimizes the location of the cryoprobes, while the cryoheaters are held fixed in their locations. Next, the cryoplanner optimizes the location of the cryoheaters, while the cryoprobes are held fixed in their new locations. Figure 6(b) shows the resulting optimum configuration. Finally, Figure 6(c) shows the optimal configuration after an additional cryoheater is added. The total defect area was found to be 9.2%, 5.6%, and 4.5%, in Figures 6(a), 6(b), and 6(c), respectively.

The result of adding cryoheaters to this configuration is an 82% decrease in the outer defect area, and a 51% decrease in the overall defect area (Table II). In terms of run time, the addition of cryoheaters significantly increased the cryoplanner run time. For this example, 28 additional iterations were required to account for the addition of cryoheaters. The cryoplanner run time is primarily dependent on the number of cryoprobes, and for this prostate configuration, each bioheat simulation takes roughly 30 seconds on a Pentium 4 comput-

Table II
Summary of parametric study results.

Case No.	Target area diameter, mm	Number of cryoprobes	Number of cryoheaters	Total defect area, %	Placement grid	Figure
1	30	5	0	9.2	No	6(a)
	30	5	2	5.6	No	6(b)
	30	5	3	4.5	No	6(c)
2	30	6	0	13.3	No	7(a)
	30	6	1	6.8	No	7(b)
	30	6	3	5.4	No	7(c)
3	30	8	0	7.1	No	8(a)
	30	8	2	5.3	No	8(b)
	30	8	4	3.6	No	8(c)
4	30	6	0	12.1	Yes	9(a)
	30	6	2	10.5	Yes	9(b)
	30	6	4	10.1	Yes	9(c)
5	56	6	0	10.4	Yes	10(a)
	56	6	2	8.0	Yes	10(b)
	56	6	4	5.6	Yes	10(c)
6	56	8	0	11.1	Yes	11(a)
	56	8	2	7.6	Yes	11(b)
	56	8	4	5.5	Yes	11(c)

er, with a 2.4 GHz processor, a 533MHz front side bus, and 256 MB of PC2700 DDR memory. The software was implemented with Visual Studio 6.0 and executed under Windows XP Professional. This means that the increase in cryoplanner run time was about 14 minutes. Techniques to accelerate the simulation run time are currently being developed.

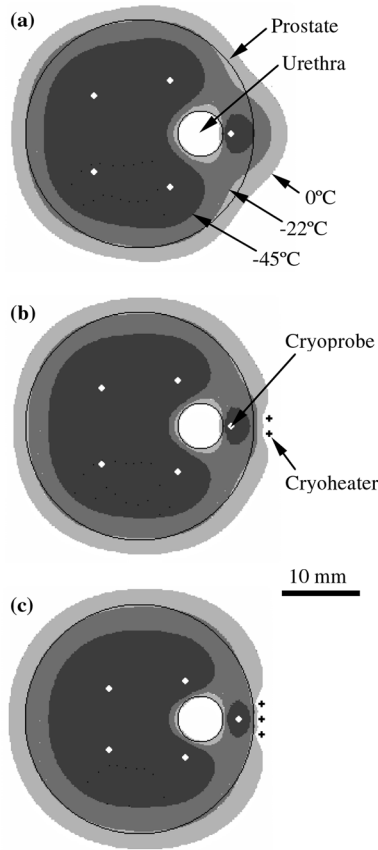


Figure 6: Planning with 5 cryoprobes and no placement grid. (a) Optimal configuration of cryoprobes resulting with 9.2% total defect area. (b) Optimal configuration of cryoprobes with two cryoheater resulting with 5.6% total defect area. (c) Optimal configuration with three cryoheaters resulting with 4.5% total defect area.

Results in Figure 6 are presented as a proof of concept, without taking into account surgical costs and medical difficulties associated with inserting the specific number of cryoheaters into the particular locations. By no means have we argue here that Figure 6(c), for example, presents the best configuration from a clinical perspective. It is optimal solely from a bio-heat transfer perspective. Ultimately, it will be up to the clinician to draw the line between the desire to improve cryosurgery outcome, and the undesired increase in cost and difficulties associated with achieving it. In the case presented in Figure 6, for example, the clinical decision may well be to use only 2 cryoheaters, as show in Figure 6(b), or even to replace them with one cryoheater, localized midway between these cryoheaters. We argue, however, that the cryoplanner can assist the clinician in making the optimal decision.

Figure 7 shows the optimization process of a typical case with 6 cryoprobes. The total defect area was found to be 13.3%, 6.8%, and 5.4%, in Figures 7(a), 7(b), and 7(c), respectively.

The end result of adding cryoheaters in this case is an 86% decrease in the outer defect area, and an overall 73% decrease in the total defect area. Here, a total of 6 iterations (including backtracking) were required to find the optimal placement with no cryoheaters, and 30 additional iterations were required to find the optimum with up to 5 cryoheaters.

It is typically assumed that the application of a larger number of cryoprobes leads to an improved outcome, measured in terms of a defect area. However, analysis of the results shown in Figures 6-8 suggests that this is not necessarily true. In the absence of cryoheaters, the application of 5 cryoprobes is superior to the application of 6 cryoprobes, and the application of 8 cryoprobes is superior to the applications of 5 and 6 cryoprobes. Compared with a 6 cryoprobe application in the absence of cryoheaters, a 5 cryoprobe application results in a 31% smaller total defect area, and an 8 cryoprobe application results in a 47% smaller total defect area. In the case of applying 2 cryoheaters, there is no significant difference between the application of 5 and 8 cryoprobes. Note that the total defect area resulting from 5 cryoprobes and 2 cryoheaters, Figure 6, is similar to the total defect area resulting from 6 cryoprobes and 3 cryoheaters, Figure 7 (summarized in Table II).

It can be seen that the application of 5 cryoprobes and 2 cryoheater (a total of 7 cryoelements) is superior to the applica-

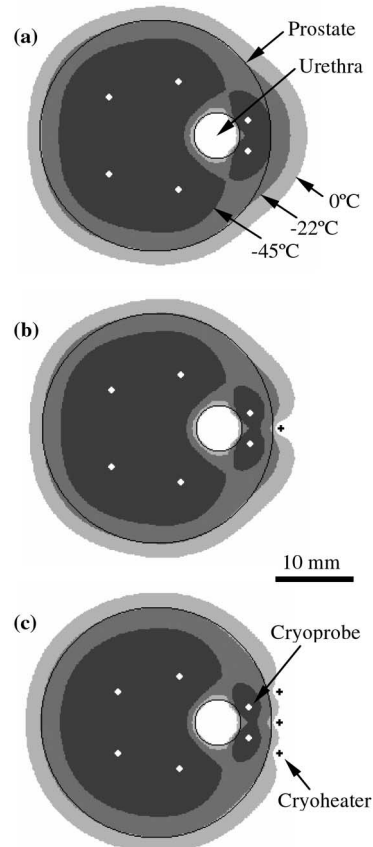


Figure 7: Planning with 6 cryoprobes and no placement grid. (a) Optimal configuration of cryoprobes resulting with 13.3% total defect area. (b) Optimal configuration of cryoprobes with two cryoheater resulting with 6.8% total defect area. (c) Optimal configuration with three cryoheaters resulting with 5.4% total defect area.

tion of 8 cryoprobcs and no cryoheaters (a total of 8 cryoelements), in terms of the total defect area. It can further be seen that the application of 5 cryoprobcs and 3 cryoheater (a total of 8 cryoelements) is superior to the application of 8 cryoprobcs and 2 cryoheaters (a total of 10 cryoelements), in terms of the total defect area. In general, an application with fewer cryoelements is expected to be more clinically desirable. Furthermore, an application with fewer cryoprobcs is easier to operate. The number of cryoheaters does not affect the ease of operation as they are designed to be self controlled.

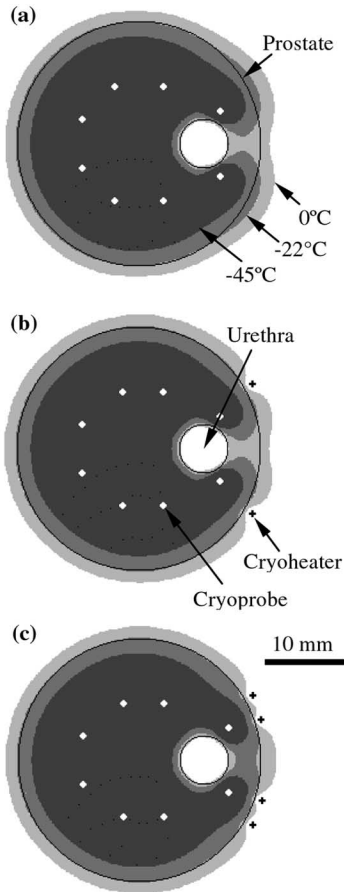


Figure 8: Planning with 8 cryoprobcs and no placement grid. (a) Optimal configuration of cryoprobcs resulting with 7.1% total defect area. (b) Optimal configuration of cryoprobcs with two cryoheater resulting with 5.3% total defect area. (c) Optimal configuration with three cryoheaters resulting with 3.6% total defect area.

Figures 9-11 present results of planning in the presence of a placement grid, where cryoelements placement is permitted in 5 mm increments only. When this constraint is applied to the simulation, a dramatic reduction in computational time is evident. Compared to the 1mm numerical simulation grid, the 5mm placement grid has 25 times fewer locations to consider during the planning process. In Figures 9-11, defects are show in black, for both interior and exterior defects.

Comparing Figures 7 and 9 illustrates the limited ability to improve planning when a placement grid is present. The entire process of optimization for the case shown in Figure 9 took only ten iterations, which roughly corresponds to 5 minutes of the cryoplanner run time. On the other hand, results

in this case are far less optimal than those in Figure 7, where no placement grid was applied. Figures 9(b) and 9(c) roughly represent the same defect area size, but a significantly different defect area shape. Most of the defect area is exterior to the target region in Figure 9(b), while most of the defect area is interior to the target region in Figure 9(c). Furthermore, a significant defect area is shown in Figure 9(c) in area to the right of the urethra. In this case the clinician would have to decide whether to permit most of the defect area to be created exterior to the target region (creating the so-called external safety margins), or to permit most of the defect area to be created interior to the target region (creating the so-called internal safety margins). Either way, the optimal configuration shown in Figure 9 is associated with large defect areas.

Comparing Figures 9 and 10 illustrates how having a larger target area makes it easier to plan because of the larger number of permitted cryoelement placement points. Furthermore, having a larger target region requires freezing to continue for a longer time. At more advanced stages of freezing, the boundary of freezing front has fewer bumps, making it easier to match the target boundary (see Fig. 2 for example).

Comparing Figures 10 and 11 indicates that the application of 6 cryoprobcs is superior to the application of 8 cryoprobcs

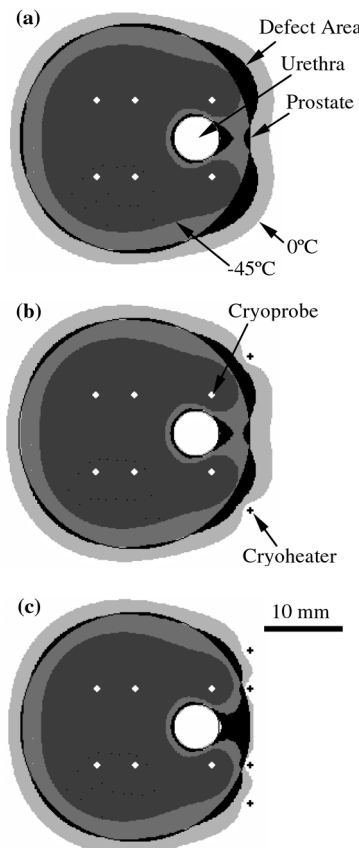


Figure 9: Planning with 6 cryoprobcs and a placement grid. (a) Optimal configuration of cryoprobcs resulting with 12.1% total defect area. (b) Optimal configuration of cryoprobcs with two cryoheater resulting with 10.5% total defect area. (c) Optimal configuration with three cryoheaters resulting with 10.1% total defect area.

in the absence of cryoheaters. The total defect area is comparable in the presence of cryoheaters, which makes the use of a larger number of cryoprobcs unnecessary.

Based on the analysis presented above, one could not conclude that more cryoprobcs lead to better cryosurgery planning in the general case, even in the absence of cryoheaters. This contradicts a common claim made by cryo-surgical device manufacturers, that an application with more cryoprobcs is superior in terms of target region coverage. In fact, this was the particular motivation to develop cryosurgical devices with more than a dozen of cryoprobcs. The cryoplanner, on the other hand, can offer the clinician with insight regarding the advantages and disadvantages of using a larger number of cryoprobcs as a starting point for the planning process.

Summary and Conclusions

The development of a new cryosurgical tool, termed a cryoheater, has been reviewed in this paper. While the application of the cryoheater is likely to improve the outcome of cryosurgery, its efficient application requires develop of a computerized planning tool. Such a tool (the cryoplanner) has been presented in this report, The cryoplanner, which can handle both cryoprobcs and cryoheaters, is a modification of a previous software prototype, which was designed for cryoprobcs only.

The goal of the cryoplanner is to identify the best locations for the cryoprobcs, and possibly cryoheaters, in order to maximize the amount of the target region that is cryoinjured, while minimizing cryoinjury external to the target region. For that purpose, a temperature isotherm for optimization was defined, with the goal of matching this isotherm with the contour of the target area. Furthermore, a defect area is defined as an area interior to the target region above this temperature isotherm, and an area exterior to the target region below this isotherm. The objective function is to reduce the total defect area in the problem. This in an optimization problem in which the objective function involves computing a sequence of bioheat transfer simulation.

The new technique is based on a force-field analogy, in which the defects apply forces to the cryoprobcs and cryoheaters, directly moving them to better locations. However, we have found that cryoprobcs and cryoheaters cannot be moved simultaneously, and an alternating procedure must be applied, in which cryoprobcs are optimized first, and cryoheaters next. The process of optimization begins without cryoheaters, which are then added in increasing numbers, until the addition of cryoheaters either does not improve the planning outcome, or the number of cryoheaters becomes too large.

Using the cryoplanner, and based on bioheat transfer simulation results, we demonstrated that that optimum planning

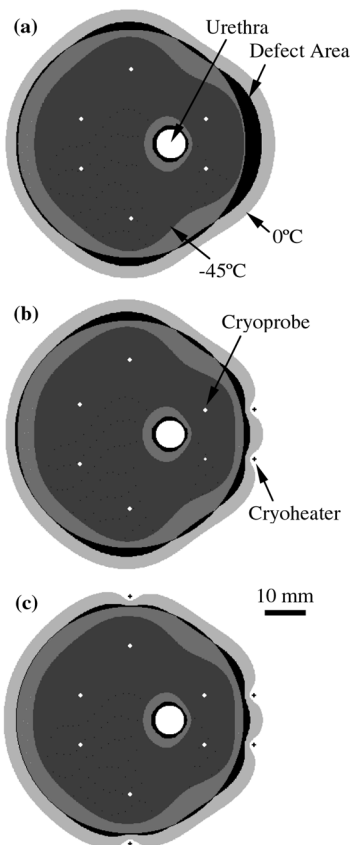


Figure 10: Planning with 6 cryoprobcs and a placement grid. (a) Optimal configuration of cryoprobcs resulting with 10.4% total defect area. (b) Optimal configuration of cryoprobcs with two cryoheater resulting with 8.0% total defect area. (c) Optimal configuration with four cryoheaters resulting with 5.6% total defect area.

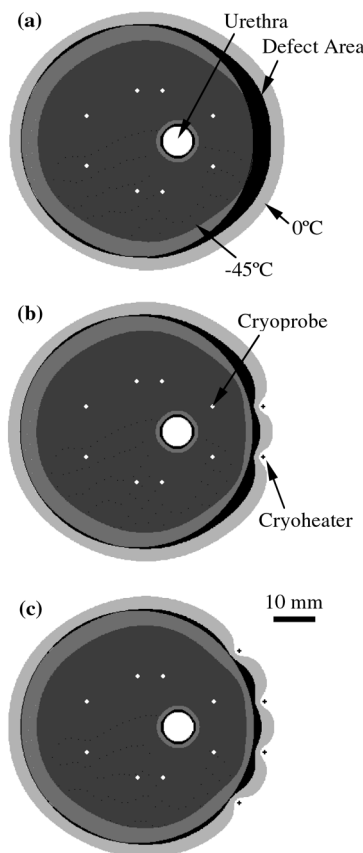


Figure 11: Planning with 8 cryoprobcs and a placement grid. (a) Optimal configuration of cryoprobcs resulting with 11.1% total defect area. (b) Optimal configuration of cryoprobcs with two cryoheater resulting with 7.6% total defect area. (c) Optimal configuration with four cryoheaters resulting with 5.5% total defect area.

can be improved with the application of cryoheaters. We further demonstrated that the common argument made by cryosurgical device manufacturer, that the an increase in number of cryoprobes improves the ability to freeze exactly the target region, is not necessarily true. Further parametric studies are currently underway.

While the objective function of minimizing the total defect area drives the process to a local optimum, other criteria should also be considered, such as the distribution of defect areas and not just the total defect area size. The goal of mathematically formulating other criteria to indicate the quality of planning is currently underway.

The potential role of cryoheaters far exceeds the simple task of minimizing the total defect area, which was demonstrated in this report. Cryoheaters could be used as a protective measure by creating a thermal barrier, in order to prevent freezing of the rectal area for example (freezing injury to this area is known to be one of the most severe complications of cryosurgery).

Finally, considering current imaging techniques, such as ultrasound and MRI, the image resolution may not be adequate to immediately terminate the cryoprocure when freezing approaches the target region boundaries. Cryoheaters, on the other hand, can help to achieve this goal to a higher degree, even when the image quality is lower.

Acknowledgement

This work has been supported in part by the Pennsylvania Infrastructure Technology Alliance (PITA), a partnership of Carnegie Mellon, Lehigh University, and the of Pennsylvania's Department of Economic Commonwealth and Community Development, grants 8039.28.1040137 and 9569.46.1040208. The cryoheater development has been supported in part by the Breast Cancer Center at the Allegheny University of the Health Sciences, Pittsburgh, PA.

References

1. Onik, G. M., Cohen, J. K., Reyes, G. D., Rubinsky, B., Chang, Z. H., Baust, J. Transrectal Ultrasound-guided Percutaneous Radical Cryosurgical Ablation of the Prostate. *Cancer* 72, 1291-1299 (1993).
2. Chang, Z., Finkelstein, J. J., Ma, H., Baust, J. Development of a High-performance Multiprobe Cryosurgical Device. *Biomed. Inst. & Tech.* 28, 383-390 (1994).
3. Lung, D.C., Stahovich, T. F., Rabin, Y. Computerized Planning of Multiprobe Cryosurgery Based on Force Field Analogy. *Journal of Computer Methods in Biomechanics and Biomedical Engineering* 7, 101-110 (2004).
4. Cohen, T. K., Miller, R. J., Shumarz, B. A. Urethral Warming Catheter for Use During Cryoablation of the Prostate. *Urology* 45, 861-864 (1995).
5. Rabin, Y., Julian, T. B., Wolmark, N. Method and apparatus for heating during cryosurgery. US Patent No. 5,899,897 (1999).
6. Rabin, Y., Stahovich, T. F. The Thermal Effect of Urethral Warming during Cryosurgery. *CryoLetters* 23, 361-374 (2002).
7. Rabin, Y., Stahovich, T. F. Cryoheater as a Means of Cryosurgery Control. *Physics in Medicine and Biology* 48, 619-632 (2003).
8. Budman, H. M., Dayan, J., Shitzer, A. Controlled Freezing of Non-ideal Solutions with Application to Cryosurgical Processes. *ASME J. Biomech. Eng.* 113, 430-437 (1991).
9. Filippi, M., Baret, C., Nourghlia, M. Hypothese de thermoreglage dans sondes pour cryoaltmologie a protoxide d'azote. The Proceedings of the 16th Int. Congress on Refrigeration, Paris, France (1983).
10. Merry, N., Smidebush, M. Apparatus for cryosurgery. US Patent 4,946,460 (1990).
11. Rabin, Y., Shitzer, A. A New Cryosurgical Device for Controlled Freezing, Part I: Setup and Validation Test. *Cryobiology* 33, 82-92 (1996).
12. Rabin, Y., Julian, T. B., Wolmark, N. A Compact Cryosurgical Apparatus for Minimal-invasive Cryosurgery. *Biomedical Instrumentation & Technology* 31, 251-258 (1997).
13. Rabin, Y., Julian, T. B., Olson, P., Taylor, M. J., Wolmark, N. Long-term Follow-up Post-cryosurgery in a Sheep Breast Model. *Cryobiology* 39, 29-46 (1999).
14. Rabin, Y., Shitzer, A. Numerical Solution of the Multidimensional Freezing Problem During Cryosurgery. *ASME J. Biomech. Eng.* 120, 32-37 (1998).
15. Gage, A. A., Baust, J. Mechanisms of Tissue Injury in Cryosurgery. *Cryobiology* 37, 171-186 (1998).
16. Rabin, Y. Uncertainty in Temperature Measurements During Cryosurgery. *CryoLetters* 19, 213-224 (1998).
17. Rabin, Y., Coleman, R., Mordohovich, D., Ber, R., Shitzer, A. A New Cryosurgical Device for Controlled Freezing, Part II: *In Vivo* Experiments on Rabbits' Hind Thighs. *Cryobiology* 33, 93-105 (1996).
18. Keanini, F. G., Rubinsky, B. Optimization of Multiprobe Cryosurgery. *Transactions of the ASME* 114, 796-801 (1992).
19. Kincaid D., Cheney, W. *Numerical Methods*, 2nd Ed. Brooks/Cole Publishing Co., Pacific Grove, CA (1996).
20. Vanderplaats, G. N. *Numerical Optimization Techniques for Engineering Design*. McGraw-Hill, New York (1984).
21. Baissalov, R., Sandison, G. A., Donnelly, B. J., Saliken, J. C., McKinnon, J. G., Muldrew, K., Rewcastle, J. C. A Semi-empirical Treatment Planning Model for Optimization of Multiprobe Cryosurgery. *Phys. Med. Biol.* 45, 1085-98 (2000).
22. Baissalov, R., Sandison, G. A., Reynolds, D., Muldrew, K. Simultaneous Optimization of Cryoprobe Placement and Thermal Protocol for Cryosurgery. *Phys. Med. Biol.* 46, 1799-814 (2001).
23. Pennes, H. H. Analysis of Tissue and Arterial Blood Temperatures in the Resting Human Forearm. *J. App. Phys.* 1, 93-122 (1948).
24. Eberhart, R. C. Thermal Models of Single Organs. In *Heat Transfer in Biology and Medicine*, pp. 261-324. Eds., Shitzer, A., Eberhart, R.C. Plenum Press, NY (1985).
25. Rabin, Y. A General Model for the Propagation of Uncertainty in Measurements into Heat Transfer Simulations and its Application to Cryobiology. *Cryobiology* 46, 109-120 (2003).
26. Altman, P. L., Dittmer, D. S. Respiration and Circulation. *Federation of American Societies for Experimental Biology (Data Handbook)*, Bethesda, MD (1971).

Date Received: February 2, 2004